The EMBO Journal (2008) 27, 2281–2292 | © 2008 European Molecular Biology Organization | All Rights Reserved 0261-4189/08
www.embojournal.org

THE EMBO JOURNAL

Δ6-Desaturase (FADS2) deficiency unveils the role of ω3- and ω6-polyunsaturated fatty acids

Wilhelm Stoffel[1,*], Barbara Holz[1], Britta Jenke[1], Erika Binczek[1], Robert Heinz Günter[1], Christine Kiss[1], Iakowos Karakesisoglou[1], Mario Thevis[2], Artur-Aron Weber[3], Stephan Arnhold[4] and Klaus Addicks[4]

[1]Center of Molecular Medicine (CMMC), Laboratory of Molecular Neurosciences, Institute of Biochemistry, University of Cologne, Cologne, Germany, [2]Institute of Biochemistry, DSHS Cologne, Cologne, Germany, [3]Department of Pharmacology, Universitätsklinikum Essen, Essen, Germany and [4]Department of Anatomy I, University of Cologne, Cologne, Germany

Mammalian cell viability is dependent on the supply of the essential fatty acids (EFAs) linoleic and α-linolenic acid. EFAs are converted into ω3- and ω6-polyunsaturated fatty acids (PUFAs), which are essential constituents of membrane phospholipids and precursors of eicosanoids, anandamide and docosanoids. Whether EFAs, PUFAs and eicosanoids are essential for cell viability has remained elusive. Here, we show that deletion of Δ6-fatty acid desaturase (FADS2) gene expression in the mouse abolishes the initial step in the enzymatic cascade of PUFA synthesis. The lack of PUFAs and eicosanoids does not impair the normal viability and lifespan of male and female fads2−/− mice, but causes sterility. We further provide the molecular evidence for a pivotal role of PUFA-substituted membrane phospholipids in Sertoli cell polarity and blood–testis barrier, and the gap junction network between granulosa cells of ovarian follicles. The fads2−/− mouse is an auxotrophic mutant. It is anticipated that FADS2 will become a major focus in membrane, haemostasis, inflammation and atherosclerosis research.

The EMBO Journal (2008) **27,** 2281–2292. doi:10.1038/emboj.2008.156; Published online 7 August 2008
Subject Categories: membranes & transport; cellular metabolism
Keywords: Δ6 fatty acid desaturase deficiency; eicosanoid deficiency; essential fatty acids; lack of PUFA synthesis; male and female sterility

Introduction

Essential fatty acid (EFA) deficiency impairs lipid and energy metabolism, polyunsaturated fatty acid (PUFA) synthesis, cell membrane structures and lipid signalling pathways and is incompatible with life (for review, see Cunnane, 2003). Mammalian cells transform the two EFAs linoleic and α-linolenic acids in a sequence of desaturation and chain elongation reactions into C20 and C22—and very long-chain (C28–C34) PUFAs (Sprecher *et al*, 1995). Arachidonic (ω6–20:$4^{5,8,11,14}$) (AA), eicosapentaenoic (ω3–20:$5^{5,8,11,14,17}$) (EPA) and docosahexaenoic (ω3–22:$6^{4,7,10,13,16,19}$) (DHA) acids are the major PUFA substituents of membrane phospholipids, which regulate cell membrane fluidity. Oxygenated metabolites of AA, EPA and DHA possess potent bioactivities. In the cyclooxygenase pathway, ω3- and ω6-eicosapolyenoic acids are converted to prostaglandins (PGEs), thromboxanes (TXBs) (Bergstroem *et al*, 1964; Hamberg and Samuelsson, 1974) and prostacyclins (Moncada *et al*, 1976), and in the linear lipoxygenase pathway to 5-hydroxy-eicosatetraenoic acid, leukotrienes and lipoxins (Samuelsson, 1981; Serhan *et al*, 1984). Moreover, ω3-DHA is converted to docosanoids (resolvins and neuroprotectins), which cause a myriad of pharmacological reactions (Taylor and Morris, 1983; Serhan *et al*, 1984, 2004). Except in reproductive organs, eicosanoids are generated in response to injury and inflammation (Ferreira, 1972; Williams, 1983).

Δ6-Fatty acid desaturase (FADS2) (Cho *et al*, 1999) catalyses the initial, rate-limiting desaturation of linoleic (ω6–18:$2^{9,12}$) to γ-linolenic (18:$3^{6,9,12}$) and α-linolenic acid (ω3–18:^{9,12,15}) to stearidonic acid (18:$4^{6,9,12,15}$).

To define the complex structural and functional role of EFAs, their derived PUFAs and eicosanoids, we investigated the role of FADS2 in the genetically defined FADS2-deficient (fads2−/−) mouse. This mutant proved that only FADS2 catalyses the key reaction. FADS2 deficiency abolishes PUFA—and consequently PGE, TXB, prostacyclin and leukotriene synthesis. Surprisingly, the viability of fads2−/− mice remains unimpaired. Platelet aggregation and thrombus formation are inhibited. Male and female fads2−/− mice are sterile. Beyond composition studies of somatic and germ cells, the role of PUFAs in male and female reproduction remains elusive (for review, see Wathes *et al*, 2007). The PUFA concentration of isolated germ cell phospholipids exceeds that of SCs, which suggested a transfer of PUFAs to developing germ cells (Saether *et al*, 2003). The fads2−/− mouse unveils the pivotal role of PUFA-substituted phospholipids in establishing cell polarity, as shown here for the tight junctions (TJs) of SCs of testis and the gap junction (GJ) network between ovarian follicle cells.

Results

FADS2 (E.C.1.14.19.3) is a 52.4 kDa (444 amino acid) subunit of the cytochrome *b*5-containing trimeric complex located in the endoplasmic reticulum membranes and is ubiquitously expressed (Supplementary Figure S1) (Cho *et al*, 1999).

Targeted deletion of FADS2 expression in the mouse

The fads2−/− mouse was generated by gene targeting. The targeting vector contained a 1.9-kb 5′-fragment harbouring

*Corresponding author. Center of Molecular Medicine (CMMC), Laboratory of Molecular Neurosciences, Institute of Biochemistry, University of Cologne, Joseph-Stelzmann-Straβe 52, 50931 Cologne, Germany. Tel.: +49 221 478 6881; Fax: +49 221 478 6882; E-mail: wilhelm.stoffel@uni-koeln.de

Received: 20 February 2008; accepted: 17 July 2008; published online: 7 August 2008

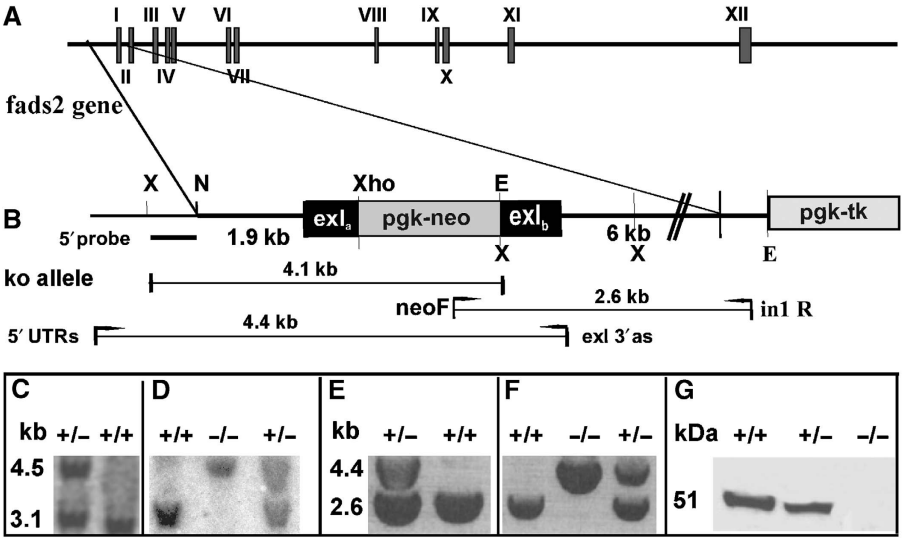

Figure 1 Generation and characterization of fads2−/− mice. (**A**) Endogenous fads2 locus. (**B**) fads2 locus disrupted by homologous recombination. Southern blot analysis of (**C**) *Xba*I-digested DNA from homologously recombined ES cells and (**D**) tail DNA. Recombined allele: 4.5-kb fragment; wt allele: 3.1-kb fragment. External probe: labelled 350-bp *Xba*I–*Pvu*II fragment. PCR of genomic DNA of (**E**) homologously recombined ES cell clone, (**F**) tail DNA of (−/−), (+/−) and wt (+/+) F1 siblings. Primers fads 5′ UTRs 5′-CCTTCCTTGTTCCAGACACGGTCTCAAGAG-3′ and reverse-primer exI end 3′ as 5′-CGTAGCATCTTCTCCCGAATAGTGTCCGAT-3′ yielded a 4.4-kb fragment for the targeted and a 2.6-kb fragment of the wt allele. (**G**) Western blot analysis of liver microsomes from wt and fads2−/− mice. Proteins were separated by gradient (4–12%) SDS–PAGE, blotted and developed by anti-FADS2 antibody (his^{329}–lys^{444}).

the 5′ sequence of exon I with the start codon deleted, and a 6-kb 3′-*Eco*RI fragment with the 3′ part of exon I, both obtained by PCR amplification of 129/SvEv mouse genomic DNA (Figure 1A and B). 129P2/Ola Hsd (HM1) mouse embryonic stem (ES) cells carrying the homologously recombined mutated fads2 allele were used for blastocyst (C57Bl/6) injection for the generation of the fads2−/− mutant mouse. ES cell (Figure 1C) and tail DNA (Figure 1D) were genotyped by Southern blot analysis and PCR (Figure 1E and F), respectively. Fads2 +/− and Fads2−/− mutant mice were viable. Fads2 is ubiquitously expressed to different degrees in wt as shown by quantitative multi-tissue RT–PCR (Supplementary Figure S1). Fads2 transcripts are absent in all fads2−/− organs. The 52.4 kDa FADS2 polypeptide was absent in western blot analysis of the liver microsomal protein fraction of fads2−/− mice (Figure 1G). Affinity-purified polyclonal antibodies, which recognize the C-terminal sequence (his^{329} to lys^{444}) of mouse FADS2, were used. Experimental details are described in Supplementary data.

FADS2 catalyses the key reaction in the conversion of EFAs to PUFAs

First, we investigated whether tissue-specific or systemic expression of redundant desaturases including fads1 and fads3 (Marquardt *et al*, 2000) could compensate for the deletion of fads2 expression. Fatty acyl substituents of neutral, phospho- and sphingolipids in total lipid extracts of liver, serum lipoproteins, ovary, testes, adrenals and retina of fads2−/− mice were analysed as methyl esters by quantitative gas–liquid chromatography–mass spectroscopy (GC/MS). Long-chain PUFAs including their main representatives 20:4, 20:5 and 22:6 proved to be absent (Table I). Mice were fed a regular diet that supplied the daily required concentration of EFAs (Supplementary Table SIII).

These results indicated that the knockout of fads2 expression prevented the processing of EFAs linoleic (ω6–18:2) and α-linolenic acid (ω3–18:3) to long-chain and very long-chain ω3- and ω6-PUFAs, and suggested that FADS2 is the only desaturase that catalyses this key step.

Key parameters of carbohydrate and lipid metabolism remain unchanged in fads2−/− mice

We then studied the impact of the disrupted synthesis of PUFAs on carbohydrate and lipid metabolism in the fads2−/− mouse. Blood glucose concentrations and glucose tolerance tests of wt and fads2−/− littermates were between 30–40 pmol/l ($n=10$) and 32–47 pmol/l ($n=10$), respectively (Supplementary Figure S2).

Parameters of lipid metabolism in age-matched wt and fads2−/− male and female cohorts ($n=12$ each) were also similar when challenged by three different diets. Total serum cholesterol of fads2−/− mice on (1) regular diet was 80 ± 12 mg/100 ml; (2) ω6-EFA-enriched diet was 110 ± 30 mg/100 ml and (3) ω3-EPA and -DHA-supplemented diet was 70 ± 10 mg/100 ml. Fatty acid compositions of these diets are summarized in Supplementary Table SII. Serum triglyceride concentrations were 180 ± 35 mg/100 ml in wt and 200 ± 20 mg/100 ml in the fads2−/− mice. The pattern of serum lipoproteins, separated and fractionated by HPLC, was assayed for total cholesterol and apolipoprotein AI distribution and proved similar in the wt and fads2−/− mice. Semiquantitative RT–PCR for key transcription factors and enzymes regulating lipid metabolism (pparα, β, γ, sreb1c, accI and fas) revealed similar steady-state concentrations in the wt and fads2−/− mice (Supplementary Figure S3). Serum leptin of fads2−/− mice ($n=5$) was comparable to that of wt littermates (2.1 ± 0.9 ng/ml).

In summary, the lack of long-chain PUFAs did not significantly affect the key parameters of lipid and carbohydrate metabolism.

Table I FADS2 deficiency abolishes PUFA synthesis

Fatty acid	Ovary		Testis		Liver		Serum		Adrenals		Retina	
	+/+	−/−	+/+	−/−	+/+	−/−	+/+	−/−	+/+	−/−	+/+	−/−
16:1	1.8	2.6	3.0	1.0		1.0	6.6	11.6	4.9	6.3	5.8	6.6
16:0	15.6	22.5	12.0	22.2	30.2	28.1	28.4	21.0	22.7	22.4	21.2	27.6
18:2	18.3	27.6	13.0	18.1	24.7	34.6	19.7	18.0	31.9	34.6	7.8	7.4
18:1	24.5	40.4	17.0	44.7	15.8	22.1	28.4	42.1	20.5	20.0	21.4	42.6
18:0	15.1	5.2	9.0	3.3	13.1	8.2	6.6	3.2	10.0	12.6	17.4	15.8
20:2		1.7				6.0		4.0	2.8	4.1		
20:4	**13.5**		**14.3**		**12.0**		**8.0**		**4.2**		**9.0**	
22:5			**11.0**									
22:6	**10.5**		**16.0**		**4.2**		**2.5**				**17.5**	
24:5	**2.7**		**2.7**						**2.9**			
26:5			**0.5**									
28:5			**0.8**									
30:5			**0.7**									

Fatty acid composition of total lipids of ovary, testis, liver, serum lipoproteins, adrenals and retina, indicating the lack of PUFAs. Mice were fed a regular diet, the fatty acid composition of which is given in Supplementary Table III.
Empty boxes: fatty acid not detectable by GLC. Mole % of PUFAs are highlighted in bold.

Eicosanoid synthesis is abolished in FADS2-deficient mice

We next investigated the role of FADS2 deficiency on eicosanoid synthesis. PGE1 and PGE2 have been first isolated from sheep vesicular glands. ω6-Dihomo-γ-linolenic (eicosatrienoic) (20:3^{8,11,14}), ω6-AA and ω3-EPA have been recognized as main precursor PUFAs (Bergstroem *et al*, 1964).

The deletion of fads2 expression causes the loss of PUFA substrates of cyclooxygenases and lipoxygenases. We examined PGE and TXB synthesis as paradigms for the cyclic cyclooxygenase pathway and leukotriene B4 (LTB4) synthesis for the linear lipoxygenase pathway. Total PGE2 concentrations in the extracts of epididymis of adult (2 months) wt and fads2−/− mice were determined by ELISA and ranged from 660 to 1100 ng per epididymis in wt ($n=10$), but only between 5 and 10 ng per epididymis in the fads2−/− male mice ($n=5$). Serum PGE2 concentrations in control mice ranged from 57 to 76 ng/ml ($n=5$) and in the fads2−/− mice from 3 to 11 ng/ml ($n=5$).

FADS2 deficiency prevents thromboembolism

TXA2 is synthesized in platelets from AA and plays a crucial role in haemostasis. TXA2 and ADP are released by platelets at the site of vascular endothelial injury and stimulate the formation of the primary haemostatic plug. Blood platelet counts were comparable in wt and in fads2−/− littermates ($n=5$), $5.88\pm0.80\times10^5$/μl and $6.22\pm0.74\times10^5$/μl, respectively. The bleeding time in the fads2−/− mice was twice as long as in wt littermates (Figure 2A). In the platelet-aggregation assay (Born, 1962; Wilner *et al*, 1968), platelets of fads2−/− mice completely failed to aggregate. They neither synthesized nor secreted TXA2, 4 versus 187 ng/ml in control mice (Figure 2B). Addition of AA rapidly restored aggregation and TXA2 synthesis and secretion by fads2−/− thrombocytes, 360 ng/ml TXA2 versus 267 ng/ml in the supernatant control platelet-enriched plasma (Figure 2C). These experiments indicated that the lack of AA acid, the precursor of TXA2, disrupted haemostasis, but cyclooxygenase and TXB synthase activities remained unimpaired.

Thrombus formation on vascular injury is a key event in the pathophysiology of several arterial diseases. To examine the response of the arterial endothelial lining at the site of injury, we used the *in vivo* murine model for acute arterial injury (Farrehi *et al*, 1998). $FeCl_3$ was topically applied to the adventitia of the common carotid artery of anaesthetized wt and fads2−/− mice. Complete thrombotic occlusion occurred in carotid arteries of the wt mice in less than 3 min (Figure 2D), whereas carotid arteries of fads2−/− mice remained free of thrombosis (Figure 2E).

Macrophages of fads2−/− mice fail to synthesize leukotrienes in immune response

At the site of inflammation, lipoxygenases of macrophages and white blood cells transform AA to leukotriene and lipoxins (Samuelsson, 1981; Serhan *et al*, 1984). We challenged LTA4/B4 synthesis in peritoneal macrophages grown in culture with lipopolysaccharide (LPS) (Akaogi *et al*, 2004), and measured LTB4 secreted into the medium by ELISA. LTB4 secretion by fads2−/− macrophages was less than 10% of that of wt macrophages, 120 ± 15 and 2200 ± 150 pg/ml, respectively, ($n=5$).

Male and female fads2−/− mice are sterile

The major phenotype of male and female fads2−/− mice is sterility. Matings of fads2−/− males and females (age 2 months) with fads2−/−, fads2+/− and wt C57BL/6 male and female, respectively, were unsuccessful. The sexual behaviour and the frequency of plug formation of fads2−/− and controls were similar. Adult (2 months) and juvenile (p15) fads2−/− males showed marked hypogonadism. Testes weight was reduced to two-third of that of age-matched wt littermates (Figure 3A–D).

During spermatogenesis, spermatogonia develop to spermatocytes and spermatids embedded in tubules formed by SCs, where they migrate from the basal to the adluminal compartment of seminiferous tubuli. Round and condensed nuclei of haploid spermatids progressively elongate and acquire acrosomal and flagellar structures. Defects in these processes lead to a lack of mature sperm cells (azoospermia),

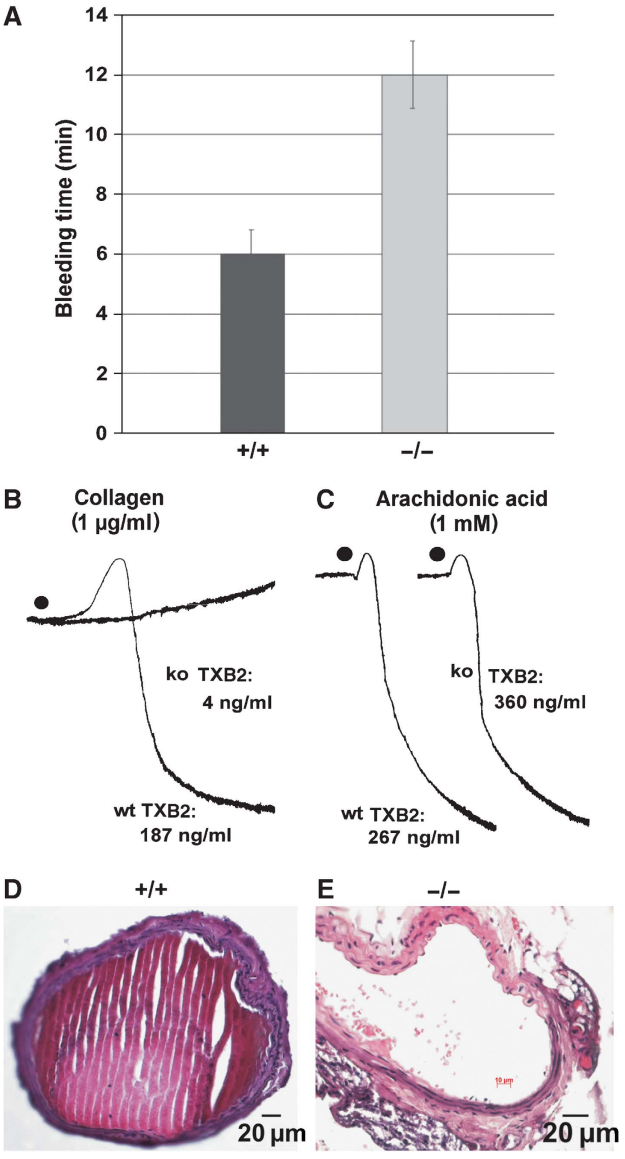

Figure 2 FADS2 deficiency and haemostasis. (**A**) Bleeding time of wt and fads2−/− mice. Tail bleeding times of wt +/+ ($n=12$) and fads2−/− littermates ($n=14$). Data represent mean ± s.e.m. (**B**) Thrombocyte aggregation assay. Platelets of wt platelet-enriched plasma of littermates aggregate immediately in response to collagen with TXA2 release (187 ng/ml). Platelets of fads−/− mice did not respond with negligible release of TXB2 (4 ng/ml). (**C**) The addition of AA restores platelet aggregation of fads2−/− thrombocytes. TXA2 release exceeds that of wt littermates (360 versus 267 ng/ml). Induction of vascular injury and thrombosis in carotid artery. (**D**) Thrombotic obliteration of the carotid artery of wt (+/+) mice ($n=10$). (**E**) Resistance to thrombosis in fads2−/− mice ($n=10$). HE-stained cross sections of +/+ and fads−/− carotid arteries.

which is a frequent cause of male infertility in the human population (Griswold, 1995; Ezeh, 2000; Gliki *et al*, 2004).

Light microscopy of sections of wt testes shows these stages of normal spermatogenesis (Figure 3E and G). Fads2−/− testes revealed SCs surrounding spermatogonia, spermatocytes I and II and haploid spermatids with round dense nuclei, which failed to complete acrosome and tail formation. The lumen of the seminiferous tubuli and the epididymis of adult fads2−/− mice lacked mature spermatozoa (Figure 3F and H). This observation was expanded

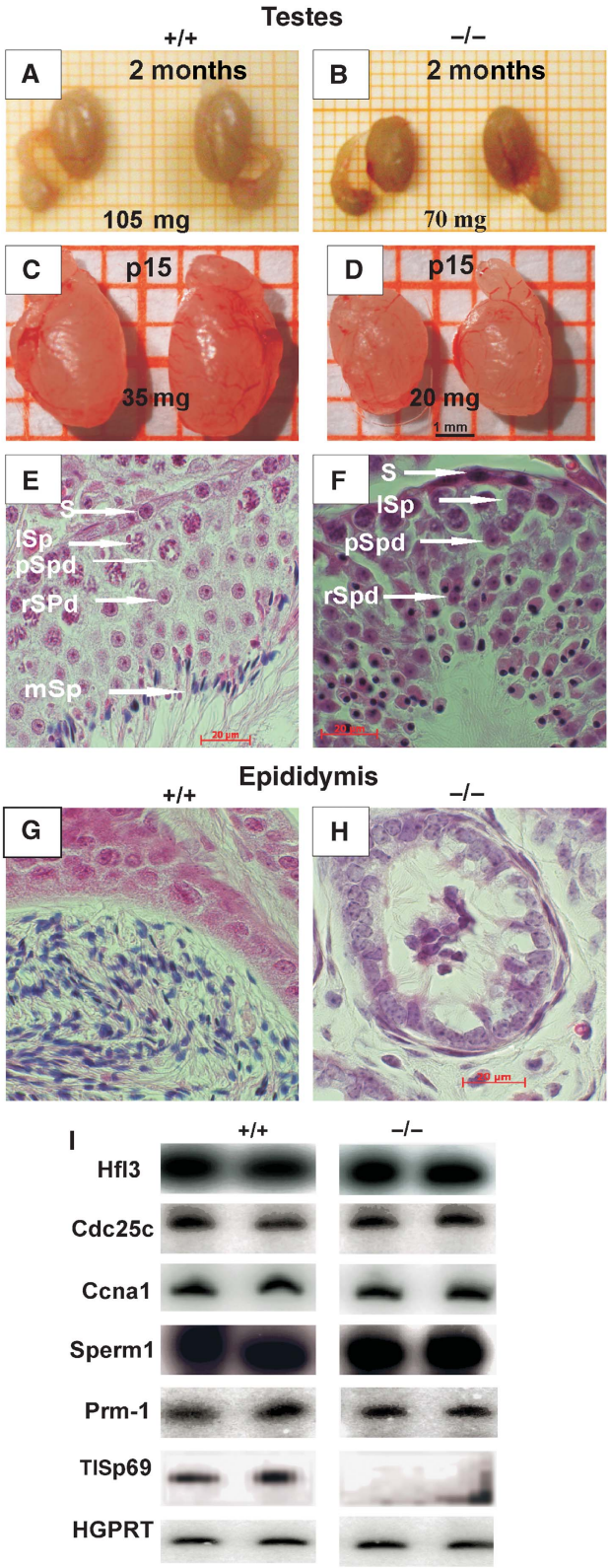

Figure 3 Pathology of testes in fads2−/− mice. Hypogonadism in age-matched fads2−/− males. Size and weight of testes and epididymis of (**A, B**) wt (+/+) and fads2−/− (−/−) mice 2mo; (**C, D**) p15 males. Arrested differentiation of spermatids of fads2−/− males. HE-stained paraffin cross-sections of (**E, F**) seminiferous tubules from wt (+/+) and fads (−/−) mice. S spermatogonia, lSp spermatocyte1, pSpd primary spermatid, rSpd round spermatid, mSP mature spermatid. (**G, H**) Epididymis of wt (+/+) and fads2−/− (−/−) mice. (**I**) Expression of stage-specific marker genes of testis during spermatogenesis measured by semi-quantitative RT–PCR.

by low- (×20) and high- (×100) resolution microscopic images of p10 and 5-month-old wt and fads2−/− testes (Supplementary Figure S5). Epididymal ductuli of adult wt males were filled with mature spermatozoa (Figure 3G), but of fads2−/− males only with detritus and immature spermatids (Figure 3H). These data suggested that spermatogenesis in fads2−/− males is arrested at the stage of round haploid spermatids.

We correlated the arrest of spermatogenesis in the fads−/− male mice with the steady-state mRNA expression level of marker genes, which are stage-specifically activated during spermatogenesis. Microarrays of testis-specific cDNA have been performed previously to study the stages of spermatogenesis (Fujii *et al*, 2002). The expression of the following marker genes was studied by semiquantitative RT–PCR: Hfl3, the testis-specific H1 histone; H1t, which is expressed in late pachytene spermatocytes (Kremer and Kistler, 1992) and cyclinA1 (Ccna1), which probes the diakinesis stage of first meiosis (Ravnik and Wolgemuth, 1999). Sperm1 is transiently expressed immediately before meiosis I in male germ cells (Andersen *et al*, 1993). Cdc25c is expressed in primary spermatocytes; Prm-1, a testis-specific mouse protamine gene, is expressed in haploid round and elongating spermatids (Kleene *et al*, 1984) and sperizin (TISP69), which functions as an E3 ligase to promote the proteasome-mediated degradation of spermatid proteins in the late spermatid stage. Only the transcript of TISP69 is missing in the expression pattern; the other markers of spermatogonia development showed identical steady-state levels of their respective mRNAs in control and fads2−/− testis (Figure 3I). Oligonucleotide primers used in RT–PCR are listed in Supplementary information Table S1.

These expression patterns of wt and fads2−/− littermates complement the morphological observations. Collectively, they also indicate a normal differentiation of spermatogenic cells of fads2−/− mice until arrested at the stage of haploid spermatids. It also supports the notion of a normal development of SCs in the fads2−/− male. We monitored the differentiation state of stable markers of mature SC by immunocytochemical studies on the expression of transcription factor SOX9, located in the nucleus of mature SCs, of the androgen receptor (AR), which is expressed highest in SC, and of Wilms tumor protein (WT-1), which is expressed continuously in mature SCs (Morais da Silva *et al*, 1996; Sharpe *et al*, 2003; Chaboissier *et al*, 2004; Gao *et al*, 2006). We observed a similar expression in adult wt and fads2−/− males (Supplementary Figure S6), which makes a differentiation defect unlikely.

Disruption of the blood–testis barrier in the fads2−/− mouse

SCs are highly polarized cells. Ectoplasmic specializations TJs, GJs and adherens junctions (AJs) form the blood–testis barrier (BTB), the boundary between basolateral and apical domains in the plasma membrane of SCs, which is critical for the differentiation of spermatids into spermatozoa. During spermatogenesis, extensive restructuring occurs at the interface of basolateral plasma membrane domains of SCs (Fanning *et al*, 1998; Mitic *et al*, 2000; Cheng and Mruk, 2002; Ebnet *et al*, 2003, 2004).

The disrupted spermiogenesis in fads2−/− males suggested molecular studies on the organization of cell membrane adhesion complexes, TJ, AJ and GJ, which maintain SC polarity and function. Immunofluorescence double labelling of wt testis revealed that TJ-specific markers occludin and JAM-A were concentrated and colocalized in the basolateral part of SCs (Figure 4A), and similarly zonula occludens-1 (ZO-1) (Figure 4C) and claudin 11 (Figure 4E), GJ marker Cx43 (Figure 4G) and AJ marker β-catenin (Figure 4I). In fads2−/− testes, these TJ and GJ markers were distributed irregularly throughout the plasma membrane of SCs (Figure 4B, D, F, H and J). Wt seminiferous tubuli contained a ring of F-actin bundles in the apical junctional complex. They form a scaffold at the SC–spermatid junctions, where they contribute to the regulation of permeability (Fanning *et al*, 1998). G-actin remained at the base of SC (Figure 4K). In fads2−/− seminiferous tubuli, F- and G-actins were distributed between the basal lamella and the adluminal compartment of the tubuli (Figure 4L). L marks the lumen of the tubulus.

These data clearly indicated that the disruption of Sertoli cell polarity and BTB in fads2−/− seminiferous tubuli causes the sterility of fads2−/− male mice.

Furthermore, electron microscopy (EM) of the BTB between adjacent SC plasma membranes of wt and fads2−/− mice (Pelletier and Byers, 1992) revealed well-structured TJ in wt (Figure 5A and B), which occlude the intercellular space between adjacent SC plasma membranes. fads2−/− SCs lack these ordered structures (Figure 5C and D).

We next investigated the steady-state expression of TJ, GJ and AJ marker proteins JAM-A, Cx43 and β-catenin of wt and fads2−/− testis by western blot analysis (Figure 4M). Their signal intensities were comparable. This suggested an unaltered gene expression of these integral membrane proteins in fads2−/− testis, independent of the disruption of the BTB, in accordance with the immunofluorescence and ultrastructural studies.

We assessed the tightness of the BTB in wt and fads2−/− testis functionally by perfusion with (a) lanthanum nitrate (Mann *et al*, 2003) and (b) the fluorescence dyes Hoechst and dextran rhodamine B, which monitor the size-selective permeation of TJ (Nitta *et al*, 2003). EM of perfused wt testis showed the interruption of the lanthanum lining between plasma membranes of SC at the TJs. In fads2−/− testis, however, lanthanum diffused freely between SC into the germ cell layers (Figure 5E and F).

The two markers Hoechst dye and dextran rhodamine B did not permeate the BTB of SCs in wt males, but in the mutant, diffusion through the basolateral compartment and the apical compartment of SCs surrounding the germ cells occurred within 5 min after the perfusion (Figure 5G and H).

The dominant PUFAs of wt testes are ω6–20:4, ω3–22:4 and ω3–22:6, which substitute the 2-position of phospholipids. Table I indicates that one-third of all fatty acids of phospholipids are eicosa- and docosapolyenoic acyl groups. They are absent in fads2−/− testes and replaced by more saturated and shorter chain acyl groups (16:1, 18:1 and 18:2). Our results suggest that the restructuring of SC–SC and SC–germ cell junction in the membrane lipid bilayer matrix during spermatogenesis is highly dependent on phospholipid species substituted with long-chain PUFAs.

Folliculogenesis is disrupted in fads2−/− females

Ovaries of wt and fads2−/− adult (Figure 6A and B) and p30 females (Figure 6C and D) also differed in size. wt ovaries

showed a strong blood supply during the cycle, which was never observed in the fads2−/− ovary. Local intercellular signalling initiates the proliferation of granulosa cells to a stratified multilayer, the formation of the zona pellucida and oocyte maturation. An intact zona pellucida is essential for fertility. Mice lacking a zona pellucida are sterile (Rankin *et al*, 1996). The multilayer syncytium of granulosa cells of preantral and antral follicles is connected by connexin43 containing GJ channels. Cx43 is expressed from the onset of folliculogenesis after birth, persists through ovulation and is required for continuous follicle growth (Hirshfield, 1991; Ackert *et al*, 2001).

The multilayer granulosa cell syncytium, theca folliculi and zona pellucida of wt ovary (Figure 6E and G) were absent in the ovaries of fads2−/− females, with the zona pellucida either absent or poorly developed and the folliculogenesis was arrested (Figure 6F and H, arrows). The dismorphic follicles in the fads2−/− ovary led us to investigate the GJ network of wt (Figure 6I) and fads2−/− (Figure 6J) granulosa cell syncytium by immunohistochemistry using Cx43 as GJ markers. Different from the regular Cx43 pattern in wt (Figure 6I), the Cx43-containing GJ channel system was completely disordered (Figure 6J). We further confirmed these observations by EM. GJs were hardly detectable in plasma membranes of adjacent granulosa cells in the fads2−/− ovary (Figure 6K–N).

Western blot analysis of wt and fads2−/− ovary protein extracts using anti-Cx43 antibodies revealed no significant difference in the signal intensity of Cx43 (Figure 6O).

Lipid polarity in Sertoli cell membrane is disturbed

Segregation of the cholesterol and the complex phospho- and sphingolipids into domain structures is essential for the maintenance of cell polarization.

In polarized cells, cholesterol, sphingomyelin and glycosphingolipids segregate into the apical cell membrane, whereas phospholipid–cholesterol-poor domains remain in the basolateral compartment. We attempted to visualize the lipid domain structure in polarized SCs of wt and fads2−/− testis by fluorescence studies using filipin, a high-affinity ligand of cholesterol in cell membranes. In cryosections of wt and fads2-null testes, treated with filipin, the fluorescent filipin–cholesterol complex was concentrated in the

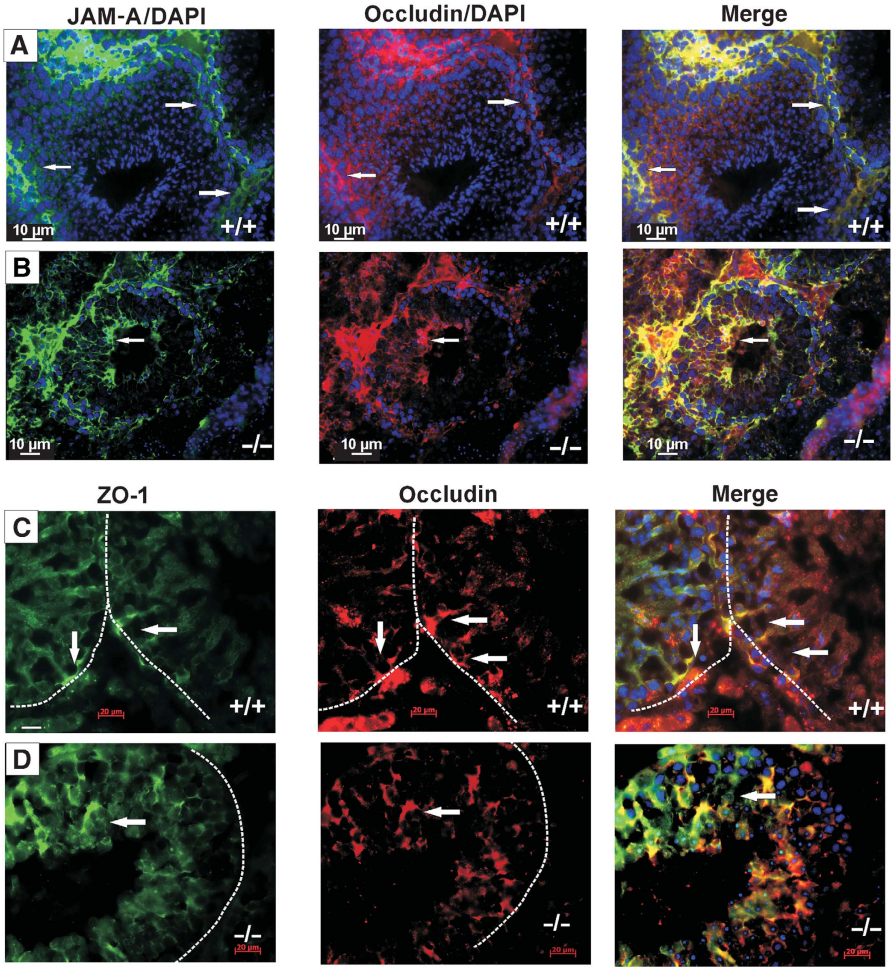

Figure 4 Disruption of the blood–testis barrier in fads2−/− males. Confocal images of cryosections of seminiferous tubuli of adult (2 months) wt and fads2−/− littermates. Double immunofluorescence labelling of TJ: (**A**, **B**) JAM-A (anti-rabbit IgG Alexa 488, green) and occludin (anti-goat IgG Cy3, red), (**C**, **D**) ZO-1 (green) and occludin, (**E**, **F**) claudin 11 (green) and occludin, stained with their respective antibodies using DAPI nuclear staining. (**G**, **H**) Anti-Cx43, (**I**, **J**) adherent junctions with anti-β-catenin antibodies (red) and TO-PRO-3 (blue) for nuclear staining. (**K**, **L**) G-actin stained with anti-G-actin antibodies (green) and F-actin with phalloidin (red). Dashed white lines mark the basal lamina. Magnification × 63. (**M**) Western blot analysis and densitometric quantification of TJ-specific JAM-A, GJ Cx43 and AJ β-catenin in the protein extracts of wt and fads2−/− testes. β-Tubulin was used as a loading marker. Arrows highlight the important changes.

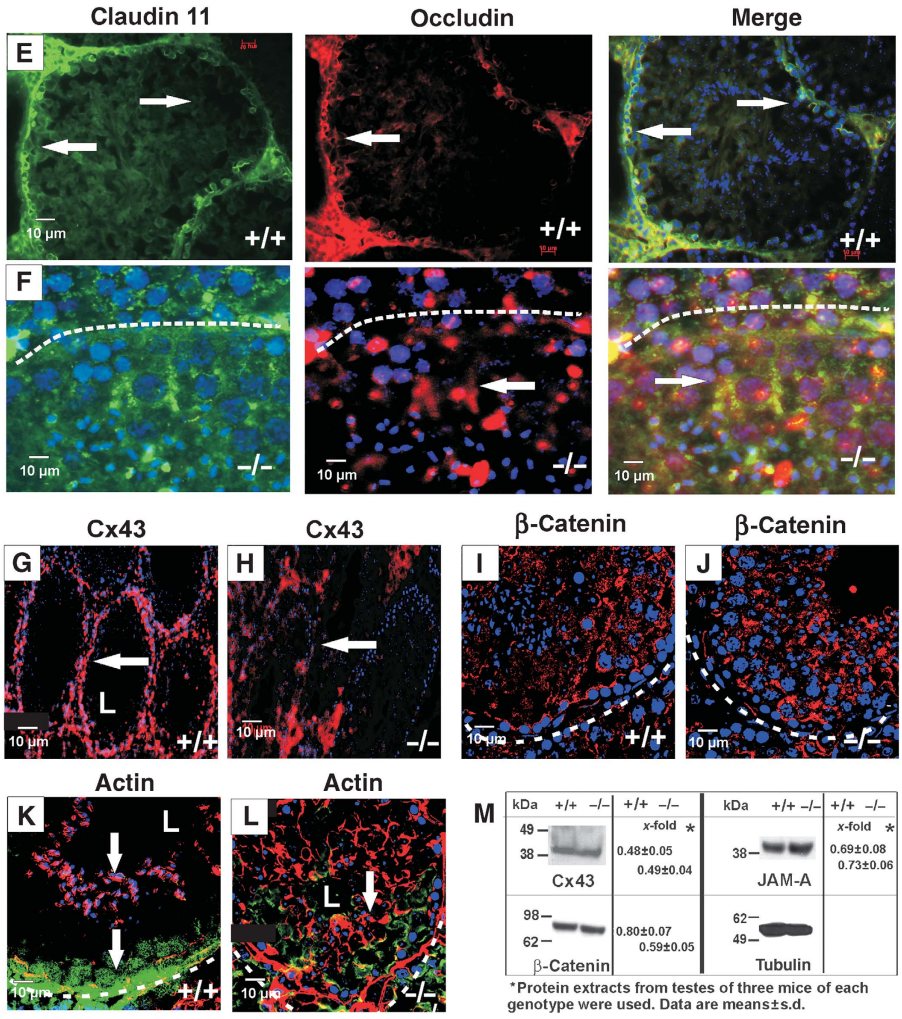

Figure 4 Continued.

adluminal domain of wt SCs (Supplementary Figure S8A), whereas in fads2−/− testis, the filipin–cholesterol complex was distributed throughout the basolateral and apical compartments (Supplementary Figure S8B).

The testis and ovary are extraordinary organs with respect to their PUFAs. The transformation of EFAs to PUFAs mainly occurs in SCs, which highly express desaturases scd1 and 2 and fads1 (Δ5) and fads2 (Δ6) (Saether *et al*, 2003). PUFA concentration of isolated germ cell phospholipids exceeds that of isolated SCs, which indicates a transfer of PUFAs to developing germ cells. During differentiation of spermatogonia to condensed spermatids, ω6–22:5 increases 10-fold and ω3–22:6 2-fold. The concomitant increase in membrane fluidity in spermatids is believed to be essential for proper motility of spermatozoa (Nolan and Hammerstedt, 1997).

Fatty acid analyses of lipids of wt and fads2−/− ovary differed dramatically: the most representative PUFAs in wt ovary are ω6–20:4, ω3–20:5 and ω3–22:6, all of which are missing in membrane phospholipids in the ovaries of fads2−/− female mice (Table I).

The fads2-null mutant is an auxotrophic mutant

The regular diet of wt and fads2−/− mice provided the daily requirement of EFAs, AA and EPA (Supplementary Table SIII), which was insufficient to reverse the fads2−/− complex phenotype. We attempted to overcome the genetic defect by daily oral administration of either a ω6–20:4 (AA) (10 mg/day) or a ω3–20:5/22:6 (EPA/DHA)-supplemented diet (Supplementary Table SIII) to cohorts of pregnant fads2+/− females ($n=10$ each), mated with fads2+/− males, and subsequently to their fads2−/− F1 male and female offsprings until maturity. Crossing these fads2−/− genders with fertile fads2+/− males and females yielded fads2−/− and fads2+/− offsprings with Mendelian distribution as shown by genotyping by PCR analysis of tail DNA of progeny of two mating experiments with fads2−/− mice fed a ω3–20:5/22:6-rich diet (Supplementary Figure S9A). GC-MS analyses of the fatty acid composition of total lipid extracts of liver, testis and ovary indicated that the *ab ovo* dietary supply of ω6–20:4 (AA) and ω3–20:5/22:6 (EPA/DHA) had restored the fatty acid pattern in membrane lipids highly enriched with long-chain PUFAs (Supplementary Table SIV and SV). Spermatogenesis in fads2−/− male and a regular follicle development in the fads2−/− female mice had been rescued. They successfully fertilized wt as well as ω3–20:5/22:6-fed fads2+/− females and yielded 7±3 siblings per crossing ($n=10$). fads2−/− females ($n=10$) on the ω3-PUFA-supplemented diet, mated with wt or fads2+/− males, gave birth to 8±3 offsprings. Litters of ω6–20:4-fed fads2−/− females were smaller ($n=4\pm2$).

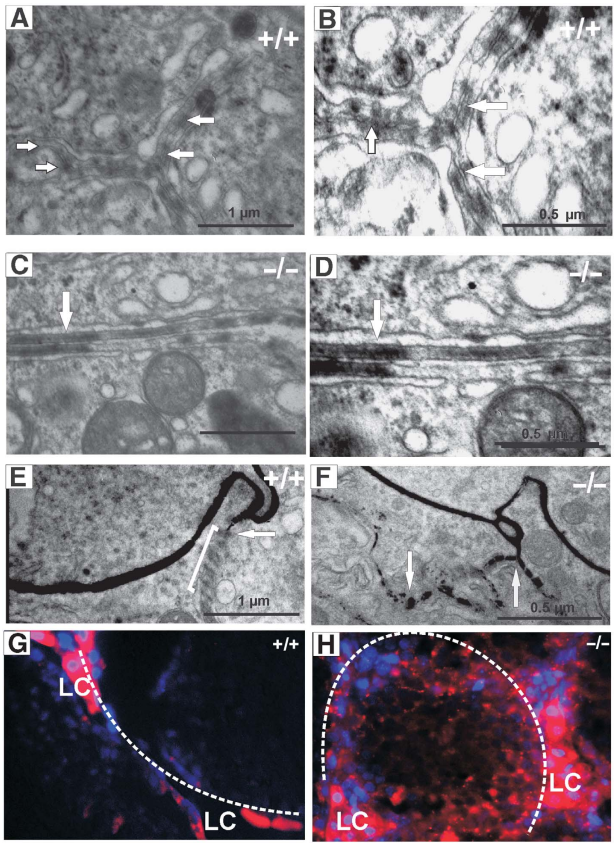

Figure 5 Ectoplasmic specialization between adjacent wt and fads2−/− SCs. (**A**) Electron micrographs of TJ in wt SCs (×30 000) and (**B**) ×50 000, (**C**) of fads2−/− SCs ×30 000 and (**D**) ×50 000. TJs close the intercellular cleft between adjacent SCs. (**E**, **F**) BTB of SC is leaky to lanthanum, which diffuses between plasma membranes of SCs of fads2−/− testis (arrows). Leakiness of BTB to immunofluorescence markers. Cryosections (10 μm) of testes of (**G**) wt and (**H**) fads2−/− adult (2 months) males after administration by cardiac perfusion of Hoechst 33258 (blue) and dextran tetramethylrhodamine (10 kDa) (fluoro-ruby) (red). LC, Leydig cells.

Light microscopy of haematoxylin–eosin (HE)-stained sections of testes of wt and PUFA-fed fads2−/− mice also revealed the rescue of spermatogenesis. The lumen of the seminiferous and epididymal tubular systems of wt and fads2−/− testes (Supplementary Figure S9B–I) were filled with spermatozoa in the fads2−/− mice (Supplementary Figure S9B–I).

Histological sections of wt ovaries (Supplementary Figure S9J and K) and fads2−/− mothers, fed with a 20:4- or 20:5/22:6-supplemented diet documented the rescue of folliculogenesis by numerous normal antral, preovulatory, secondary and tertiary follicles with zona pellucida (Supplementary Figure S9L and M).

AA-supplemented diet rescued eicosanoid synthesis in the fads2−/− mice. Normal bleeding time, platelet aggregation and rapid thrombotic occlusion of the injured carotid artery (Supplementary Figure S10A–C) were restored. Also, leukotriene synthesis and secretion by LPS-stimulated peritoneal macrophages of 20:4-fed fads2-null foster mothers and homozygous siblings were normalized. The bleeding time of 20:5/22:6-fed fads2−/− mice, platelet aggregation and the rapid thrombotic occlusion of the injured carotid artery were not normalized (data not shown).

Discussion

EFA deficiency impairs lipid and energy metabolism, PUFA synthesis, cell membrane structures and lipid signalling pathways, and is incompatible with life (Cunnane, 2003). Despite studies in a large variety of feeding experiments in different mammalian species, the decade-old question of the role of EFAs, of long-chain PUFAs or the eicosanoids in mammalian cell viability has remained elusive. The fads2−/− mouse model permits for the first time well-defined studies on the separate roles of the ω3- and ω6-EFAs, individual PUFAs and eicosanoids, for which the studies reported here have advanced our understanding in four key areas.

First, the development and viability of FADS2-deficient mice are independent of long-chain PUFAs and eicosanoids. Second, among the members of the two families of desaturases, the five Δ9-desaturases (SCD1–5) (Ntambi *et al*, 2004; Binczek *et al*, 2007) and three desaturases of the fads family: fads1 (Δ5-desaturase), fads2 (Cho *et al*, 1999) and fads3 (Marquardt *et al*, 2000), only FADS2 initiates the desaturation-chain elongation cascade, by which EFAs are transformed to ω3- and ω6-PUFAs. Loss of fads2 expression in the fads2-null mouse, characterized here, abolishes the synthesis of long and very long-chain polyenoic acids. Third, the absence of dihomo-γ-linolenic (20:3^{8,11,14}), AA and EPA in the fads2−/− mouse deprives the cyclooxygenase and lipoxygenase pathways from their substrates, which we demonstrated with three paradigms, for the cyclooxygenase pathway (a) by the elimination of PGE synthesis in the epididymis, (b) the failure of synthesis of TXBs by thrombocytes, in the platelet aggregation assay and the resistance of the endothelial lining of the common carotid artery to thromboembolism. (c) In the linear lipoxygenase pathway, LPS-stimulated peritoneal macrophages of fads2−/− mice failed to synthesize leukotrienes. Fourth, FADS2 deficiency causes hypogonadism and sterility of male (azoospermia) and female mice. Cessation of spermatogenesis in male fads2−/− mice occurs at the stage of round spermatids and leads to azoospermia, which is frequently caused by a disrupted BTB. BTB is formed by TJ and AJ protein complexes confined to the basolateral compartment of highly polarized SCs (Fanning *et al*, 1998; Chapin *et al*, 2001; Ebnet *et al*, 2003). Two main integral membrane proteins with four membrane-spanning domains (TMDs) are occludin and claudin11 and the single TMD protein JAM-A. They reside in the TJ complexes of the plasma membrane and form scaffolds for intracellular binding partner, for example, ZO-1 and Par3 (Ebnet *et al*, 2003).

Our immunohistochemical studies revealed that occludin, claudin11, JAM-A and ZO-1, GP protein Cx43 and also AJ protein β-catenin were dislocated throughout the basolateral and apical compartments of the fads2−/− SC plasma membrane, indicating the breakdown of the BTB. In wt mice, G-actin is located basolaterally and F-actin bundles are concentrated in the adluminal domain of SC. Here, they form a scaffold at the Sertoli–spermatid junctions, which is essential for spermatid maturation (Fanning *et al*, 1998). In fads2−/− tubuli, however, F-actin is scattered throughout the germ cell epithelium.

Transmission EM supports the well-structured ZO between SCs, which are missing in fads2−/− testes (Figure 5A–D).

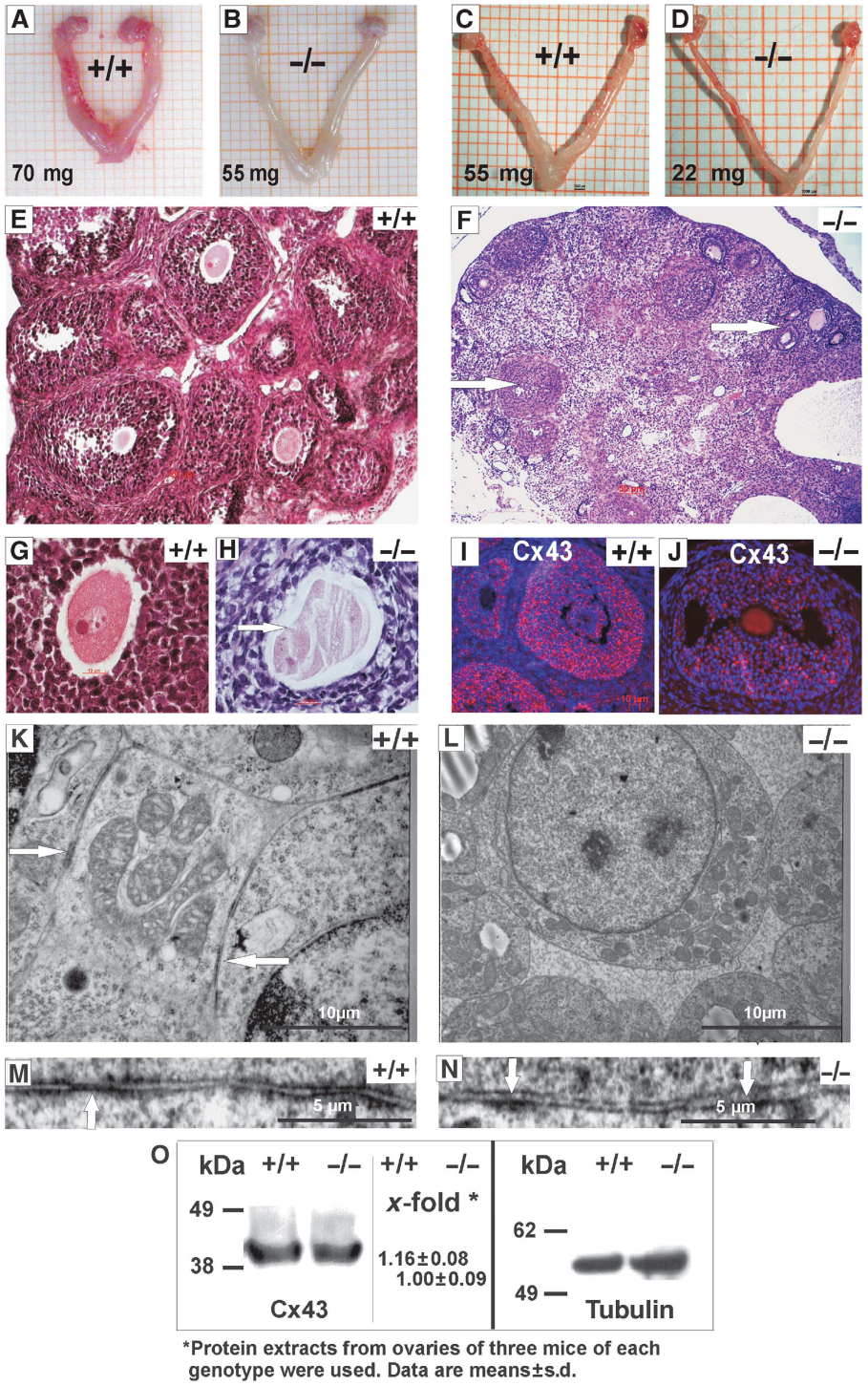

Figure 6 Hypogonadism and follicle atresia of fads2−/− females. Genital tract of (**A**, **B**) wt (+/+) and fads2−/− (−/−) adult mice and (**C**, **D**) of p30 mice. Cross sections of wt (+/+) and fads2−/− (−/−) ovaries. (**E**, **G**) wt ovary and follicle, (**F**, **H**) atretic follicle (arrow), disordered follicle cell layers, degenerated ovum, undeveloped zona pellucida (arrow). The GJ network between granulosa cells is missing, AJs are dislocated. Confocal microscopy of cryosections (7 µm) of wt (+/+) and fads2−/− (−/−) ovaries stained with (**I**, **J**) anti-Cx43 antibodies. Second antibody Cy3-conjugated anti-rabbit IgG. (**K**, **L**) EM micrographs of granulosa cells of wt and fads2−/− ovary. Magnification: ×3000 and ×30 000 (**M**, **N**). (**O**) Western blot analysis of wt and fads2−/− ovary protein extracts probing with anti-Cx43 for GJ.

Finally, we probed the BTB functionally by two perfusion experiments. EM of wt testis perfused with lanthanum (Mann *et al*, 2003) revealed a sharp lining between adjacent Sertoli cell plasma membranes, which stopped at the impermeable TJ (BTB) (Figure 5E, arrow). The BTB of fads2−/− mice became leaky and lanthanum diffused between adjacent SCs (Figure 5F, arrows).

In perfusion experiments with fluorescent dextran tetramethylrhodamine (10 kDa), TJ between wt SC membranes remained impermeable, but became rapidly leaky (3–5 min) in fads2−/− testis.

Ovaries of the infertile adult (2 months) fads2−/− females show numerous dysmorphic follicles. Studies on the role of GJ in folliculogenesis revealed that Cx43 is expressed from

the onset of folliculogenesis after birth and is required for continuous follicle growth (Hirshfield, 1991; Ackert *et al*, 2001). The multilayered granulosa cell syncytium of preantral and antral follicles of wt female mice is connected by an extensive network of GJs, which is disordered and scarcely developed in the fads2−/− ovary, as shown by immunofluorescence using anti-Cx43 antibodies.

In the ovaries of wt and fads2−/− mice, the steady-state concentrations of junction-specific Cx43 mRNA, as well as the Cx43 protein and testis of β-catenin, occludin and JAM-A, are similar. They differ only in the lack of PUFA-substituted membrane phospholipids in the fads2−/− mouse. This substantiates the notion that the absence of PUFAs in phospholipids of the plasma membrane lipid bilayer of SCs, germ cells and granulosa cells causes the structural disruption of the plasma membrane junction systems and consequently sterility of both male and female fads2−/− mice.

PUFA deficiency prohibits segregation into lipid domains in fads2−/− SC plasma membranes

TJ demarcates the asymmetric distribution of proteins and lipid species into distinct, immiscible basolateral and apical domains and maintain the polarity of the plasma membranes. Phospholipids are predominantly segregated into liquid-disordered domains in the basolateral, and sphingolipids and cholesterol into tightly packed domains of the apical compartment (Brown and London, 1998; Simons and Toomre, 2000; Rajendran and Simons, 2005).

In highly polarized SCs of wt testes and ovary, more than one-third of the phospholipid species are substituted by C20- and C22-PUFAs, which are replaced in the fads2−/− mice by more saturated C18-acyl groups. The multiple double-bond systems of AA, EPA and DHA substituents of phospholipids confer a high degree of conformational flexibility to the lipid bilayer of the plasma membrane of SC and follicle cells, essential for the engagement and disengagement of integral membrane and adaptor protein complexes of TJ and AJ during germ cell maturation.

Compatible with the interpretation of the data reported here are NMR and X-ray studies of *in vitro* model systems, which demonstrated that the rigid cholesterol structure in the highly disordered environment of the cis-double-bond systems of PUFA-substituted phospholipids causes segregation into PUFA-rich–cholesterol-poor and sphingomyelin/cholesterol-rich microdomains in the lipid bilayer. Oleic- and linoleic acid-substituted phospholipids have a higher degree of order and affinity for cholesterol binding (Stillwell and Wassall, 2003; Wassall *et al*, 2004).

Analogously, the absence of long-chain PUFA-substituted phospholipids of fads2−/− SC plasma membrane might alter the affinity of cholesterol and thereby prohibit the segregation into apical cholesterol-sphingolipid-rich and basolateral phospholipid-rich–cholesterol-poor domains. Consequently, this would interfere with the partitioning of scaffolding proteins into TJ, AJ and GP complexes, and cause the loss of SC polarity.

We visualized the localization of cholesterol in the plasma membrane of SCs with filipin, a widely used high-affinity fluorescent ligand of cholesterol (for review, see Brown and London, 1998; Orlandi and Fishman, 1998; Eisenberg *et al*, 2006). In SCs of wt testis, fluorescent cholesterol–filipin complexes were concentrated in the apical domain but randomly distributed in SCs of fads2−/− seminiferous tubuli (Supplementary Figure S8A and B).

These data are consistent with the proposition that PUFA-rich phospholipid–cholesterol-poor microdomains provide the molecular platform for the permanent reconstruction of the membrane and adaptor protein complexes of TJ, GJ and AJ during germ cell maturation and movement.

We have initiated studies on the impact of FADS2 deficiency on cell polarity of other polarized epithelial cells, notably enterocytes and ciliated epithelial cells of the trachea. Immunofluorescence studies on enterocytes of jejunum using antibodies recognizing occludin and clathrin 11, and podocin as a marker for trachea epithelial cells revealed no perturbation of their TJ systems (Supplementary Figure S7).

Retinal photoreceptors contain abundant DHA in membrane phospholipids. Preliminary results of EM studies indicated severe structural changes in the interphase between retinal pigment epithelium and the neuroepithelial photoreceptor layer (data not shown), which await further molecular clarification.

Materials and methods

Targeting the fads2 gene

The targeting construct was generated by the insertion of a 5′ 1.9-kb *Not*I–*Xho*I fragment with a 5′ homology of exon I as short arm adjacent to the 5′-end of the pgk-neo expression cassette and a 6-kb *Eco*RI fragment as 3′ long arm with 3′ homology, consisting of the 3′ sequence of exon I and intron 1, followed by the thymidine kinase gene (pgk-tk) outside the genomic sequence, allowing positive/negative selection (Figure 1A and B). The cloning strategy for the targeting vector, electroporation of ES cells, clone selection, genotyping and blastocyst injection have been described before (Bradley *et al*, 1984). Breeding of germline-transmitting chimaeric males to homozygozity and genotyping by PCR of genomic DNA are outlined in Supplementary data.

Expression studies

The expression of FADS2 in different tissues of the fads2−/− mouse was estimated by semiquantitative RT–PCR of multi-tissue RNA (liver, kidney, brain, spleen, muscle, heart, intestine and white adipose tissue) as described in Supplementary data.

Laboratory measurements

Plasma cholesterol, triglycerides, LDL and HDL cholesterol were determined by standard colorimetric assays. Serum lipoproteins were separated by FPLC using a Superose-6 FPLC column as described in Supplementary data. Lipoproteins were separated by agarose gel electrophoresis (1% agarose in 10 mM Tris, pH 8.6) and transferred to a nitrocellulose membrane by capillary blotting and apolipoprotein (apo) AI were detected by western blot analysis.

Lipid analysis

Isolation, fractionation and identification of lipids from liver, brain, kidney, testis, ovary and muscle and of their fatty acid substituents are described in detail in Supplementary data.

Western blot analysis

Western blot analysis of wt and fads2−/− liver microsomal proteins is described in Supplementary data.

Quantification of eicosanoids

TXB2, PGE E2 and LTB4 were quantified by ELISA using the enzyme Immunoassay Kit Correlate EIA TXB2, LTB4 and PGE2 (Assay Designs Inc., Ann Arbor, MI, USA).

Bleeding time and platelet aggregation assay

Bleeding time was measured by trans-section of the mouse tail of anesthetized wt and fads2−/− mice at about 2 mm diameter, and the bleeding time was determined with the tail inserted in a glass

beaker filled with saline at 37°C. The mouse was placed on a 30°C heat pad. The bleeding time was recorded for 30 min.

Induced arterial thrombosis

Arterial thrombosis was induced using 5% $FeCl_3$ following the procedure as described previously (Farrehi *et al*, 1998). Thrombosis was documented in cross sections of the common carotid artery of wt and fads2−/− mutant, stained with HE.

Peritoneal macrophage stimulation assay and measurement of leukotriene synthesis in unstimulated and stimulated macrophages are described in Supplementary data.

Histology and immunohistochemistry

Two-month-old wt, hetero- and homozygous fads2 mice were perfused from the left ventricle with PBS and PBS-buffered 4% paraformaldehyde and organs were fixed for cryo- or paraffin embedding. Processing of sections for light- and immunofluorescence microscopy is described in Supplementary data.

EM was carried out as described in Supplementary data.

TJ permeability

Mice were perfused from the left ventricle with Hoechst 33258 pentahydrate (bisbenzimide) (blue) and dextran tetramethylrhodamine (10 000 MW) (fluoro-ruby) (red) (Invitrogen Molecular Probes, Eugene, OR, USA) as described before (Mann *et al*, 2003; Nitta *et al*, 2003) and cryosections (10 μm) of testes of wt and fads2−/− adult (2 months) males were analysed by immunofluorescence. Ultrathin sections of lanthanum-perfused testes were studied by EM (Supplementary data).

Feeding experiments

Feeding experiments with EFAs, ω3- and ω6-PUFA-supplemented diets are described in Supplementary data.

Hormone determination

Serum testosterone and estradiol of adult control and fads2−/− male and female littermates, respectively, were determined by ELISA using the Immunoassay Kit Correlate EIA (Assay Designs Inc.).

Supplementary data

Supplementary data are available at *The EMBO Journal* Online (http://www.embojournal.org).

Acknowledgements

This study was supported by the Center of Molecular Medicine Cologne. We thank K Willecke, Institute of Genetics, University of Bonn, for providing Cx43 antibodies; K Ebnet, Institute of Cell Biology, University of Münster, for anti JAM-A and C antibodies and K Schroer, Institute of Pharmacology, University of Düsseldorf, for the thromboxane RIA analyses. Experiments were carried out in accordance with the guidelines of the Ethics Committee of the Faculty of Medicine, University of Cologne.

Conflict of interest

The authors declare that they have no competing financial interests.

References

Ackert CL, Gittens JE, O'Brien MJ, Eppig JJ, Kidder GM (2001) Intercellular communication via connexin43 gap junctions is required for ovarian folliculogenesis in the mouse. *Dev Biol* **233:** 258–270

Akaogi J, Yamada H, Kuroda Y, Nacionales DC, Reeves WH, Satoh M (2004) Prostaglandin E2 receptors EP2 and EP4 are up-regulated in peritoneal macrophages and joints of pristane-treated mice and modulate TNF-alpha and IL-6 production. *J Leukoc Biol* **76:** 227–236

Andersen B, Pearse II RV, Schlegel PN, Cichon Z, Schonemann MD, Bardin CW, Rosenfeld MG (1993) Sperm 1: a POU-domain gene transiently expressed immediately before meiosis I in the male germ cell. *Proc Natl Acad Sci USA* **90:** 11084–11088

Bergstroem S, Danielsson H, Klenberg D, Samuelsson B (1964) The enzymatic conversion of essential fatty acids into prostaglandins. *J Biol Chem* **239:** PC4006–PC4008

Binczek E, Jenke B, Holz B, Günter RH, Thevis M, Stoffel W (2007) Obesity resistance of the stearoyl-CoA deficient (scd1−/−) mouse results from disruption of the epidermal lipid barrier and adaptive thermoregulation. *Biol Chem* **388:** 405–418

Born GV (1962) Aggregation of blood platelets by adenosine diphosphate and its reversal. *Nature* **194:** 927–929

Bradley A, Evans M, Kaufman MH, Robertson E (1984) Formation of germ-line chimaeras from embryo-derived teratocarcinoma cell lines. *Nature* **309:** 255–256

Brown DA, London E (1998) Functions of lipid rafts in biological membranes. *Annu Rev Cell Dev Biol* **14:** 111–136

Chaboissier MC, Kobayashi A, Vidal VI, Lutzkendorf S, van de Kant HJ, Wegner M, de Rooij DG, Behringer RR, Schedl A (2004) Functional analysis of Sox8 and Sox9 during sex determination in the mouse. *Development* **131:** 1891–1901

Chapin RE, Wine RN, Harris MW, Borchers CH, Haseman JK (2001) Structure and control of a cell–cell adhesion complex associated with spermiation in rat seminiferous epithelium. *J Androl* **22:** 1030–1052

Cheng CY, Mruk DD (2002) Cell junction dynamics in the testis: Sertoli–germ cell interactions and male contraceptive development. *Physiol Rev* **82:** 825–874

Cho HP, Nakamura M, Clarke SD (1999) Cloning, expression, and fatty acid regulation of the human delta-5 desaturase. *J Biol Chem* **274:** 37335–37339

Cunnane SC (2003) Problems with essential fatty acids: time for a new paradigm? *Prog Lipid Res* **42:** 544–568

Ebnet K, Aurrand-Lions M, Kuhn A, Kiefer F, Butz S, Zander K, Meyer zu Brickwedde MK, Suzuki A, Imhof BA, Vestweber D (2003) The junctional adhesion molecule (JAM) family members JAM-2 and JAM-3 associate with the cell polarity protein PAR-3: a possible role for JAMs in endothelial cell polarity. *J Cell Sci* **116:** 3879–3891

Ebnet K, Suzuki A, Ohno S, Vestweber D (2004) Junctional adhesion molecules (JAMs): more molecules with dual functions? *J Cell Sci* **117:** 19–29

Eisenberg S, Shvartsman DE, Ehrlich M, Henis YI (2006) Clustering of raft-associated proteins in the external membrane leaflet modulates internal leaflet H-ras diffusion and signaling. *Mol Cell Biol* **26:** 7190–7200

Ezeh UI (2000) Beyond the clinical classification of azoospermia: opinion. *Hum Reprod* **15:** 2356–2359

Fanning AS, Jameson BJ, Jesaitis LA, Anderson JM (1998) The tight junction protein ZO-1 establishes a link between the transmembrane protein occludin and the actin cytoskeleton. *J Biol Chem* **273:** 29745–29753

Farrehi PM, Ozaki CK, Carmeliet P, Fay WP (1998) Regulation of arterial thrombolysis by plasminogen activator inhibitor-1 in mice. *Circulation* **97:** 1002–1008

Ferreira SH (1972) Prostaglandins, aspirin-like drugs and analgesia. *Nat New Biol* **240:** 200–203

Fujii T, Tamura K, Masai K, Tanaka H, Nishimune Y, Nojima H (2002) Use of stepwise subtraction to comprehensively isolate mouse genes whose transcription is up-regulated during spermiogenesis. *EMBO Rep* **3:** 367–372

Gao F, Maiti S, Alam N, Zhang Z, Deng JM, Behringer RR, Lecureuil C, Guillou F, Huff V (2006) The Wilms tumor gene, Wt1, is required for Sox9 expression and maintenance of tubular architecture in the developing testis. *Proc Natl Acad Sci USA* **103:** 11987–11992

Gliki G, Ebnet K, Aurrand-Lions M, Imhof BA, Adams RH (2004) Spermatid differentiation requires the assembly of a cell polarity complex downstream of junctional adhesion molecule-C. *Nature* **431:** 320–324

Griswold MD (1995) Interactions between germ cells and Sertoli cells in the testis. *Biol Reprod* **52:** 211–216

Hamberg M, Samuelsson B (1974) Prostaglandin endoperoxides. Novel transformations of arachidonic acid in human platelets. *Proc Natl Acad Sci USA* **71:** 3400–3404

Hirshfield AN (1991) Development of follicles in the mammalian ovary. *Int Rev Cytol* **124:** 43–101

Kleene KC, Distel RJ, Hecht NB (1984) Translational regulation and deadenylation of a protamine mRNA during spermiogenesis in the mouse. *Dev Biol* **105:** 71–79

Kremer EJ, Kistler WS (1992) Analysis of the promoter for the gene encoding the testis-specific histone H1t in a somatic cell line: evidence for cell-cycle regulation and modulation by distant upstream sequences. *Gene* **110:** 167–173

Mann MC, Friess AE, Stoffel MH (2003) Blood–tissue barriers in the male reproductive tract of the dog: a morphological study using lanthanum nitrate as an electron-opaque tracer. *Cells Tissues Organs* **174:** 162–169

Marquardt A, Stohr H, White K, Weber BH (2000) cDNA cloning, genomic structure, and chromosomal localization of three members of the human fatty acid desaturase family. *Genomics* **66:** 175–183

Mitic LL, Van Itallie CM, Anderson JM (2000) Molecular physiology and pathophysiology of tight junctions I. Tight junction structure and function: lessons from mutant animals and proteins. *Am J Physiol Gastrointest Liver Physiol* **279:** G250–G254

Moncada S, Needleman P, Bunting S, Vane JR (1976) Prostaglandin endoperoxide and thromboxane generating systems and their selective inhibition. *Prostaglandins* **12:** 323–335

Morais da Silva S, Hacker A, Harley V, Goodfellow P, Swain A, Lovell-Badge R (1996) Sox9 expression during gonadal development implies a conserved role for the gene in testis differentiation in mammals and birds. *Nat Genet* **14:** 62–68

Nitta T, Hata M, Gotoh S, Seo Y, Sasaki H, Hashimoto N, Furuse M, Tsukita S (2003) Size-selective loosening of the blood–brain barrier in claudin-5-deficient mice. *J Cell Biol* **161:** 653–660

Nolan JP, Hammerstedt RH (1997) Regulation of membrane stability and the acrosome reaction in mammalian sperm. *FASEB J* **11:** 670–682

Ntambi JM, Miyazaki M, Dobrzyn A (2004) Regulation of stearoyl-CoA desaturase expression. *Lipids* **39:** 1061–1065

Orlandi PA, Fishman PH (1998) Filipin-dependent inhibition of cholera toxin: evidence for toxin internalization and activation through caveolae-like domains. *J Cell Biol* **141:** 905–915

Pelletier RM, Byers SW (1992) The blood–testis barrier and Sertoli cell junctions: structural considerations. *Microsc Res Tech* **20:** 3–33

Rajendran L, Simons K (2005) Lipid rafts and membrane dynamics. *J Cell Sci* **118:** 1099–1102

Rankin T, Familari M, Lee E, Ginsberg A, Dwyer N, Blanchette-Mackie J, Drago J, Westphal H, Dean J (1996) Mice homozygous for an insertional mutation in the Zp3 gene lack a zona pellucida and are infertile. *Development* **122:** 2903–2910

Ravnik SE, Wolgemuth DJ (1999) Regulation of meiosis during mammalian spermatogenesis: the A-type cyclins and their associated cyclin-dependent kinases are differentially expressed in the germ-cell lineage. *Dev Biol* **207:** 408–418

Saether T, Tran TN, Rootwelt H, Christophersen BO, Haugen TB (2003) Expression and regulation of delta5-desaturase, delta6-desaturase, stearoyl-coenzyme A (CoA) desaturase 1, and stearoyl-CoA desaturase 2 in rat testis. *Biol Reprod* **69:** 117–124

Samuelsson B (1981) Leukotrienes: mediators of allergic reactions and inflammation. *Int Arch Allergy Appl Immunol* **66** (Suppl 1)**:** 98–106

Serhan CN, Gotlinger K, Hong S, Arita M (2004) Resolvins, docosatrienes, and neuroprotectins, novel omega-3-derived mediators, and their aspirin-triggered endogenous epimers: an overview of their protective roles in catabasis. *Prostaglandins Other Lipid Mediat* **73:** 155–172

Serhan CN, Hamberg M, Samuelsson B (1984) Lipoxins: novel series of biologically active compounds formed from arachidonic acid in human leukocytes. *Proc Natl Acad Sci USA* **81:** 5335–5339

Sharpe RM, McKinnell C, Kivlin C, Fisher JS (2003) Proliferation and functional maturation of Sertoli cells, and their relevance to disorders of testis function in adulthood. *Reproduction* **125:** 769–784

Simons K, Toomre D (2000) Lipid rafts and signal transduction. *Nat Rev Mol Cell Biol* **1:** 31–39

Sprecher H, Luthria DL, Mohammed BS, Baykousheva SP (1995) Reevaluation of the pathways for the biosynthesis of polyunsaturated fatty acids. *J Lipid Res* **36:** 2471–2477

Stillwell W, Wassall SR (2003) Docosahexaenoic acid: membrane properties of a unique fatty acid. *Chem Phys Lipids* **126:** 1–27

Taylor GW, Morris HR (1983) Lipoxygenase pathways. *Br Med Bull* **39:** 219–222

Wassall SR, Brzustowicz MR, Shaikh SR, Cherezov V, Caffrey M, Stillwell W (2004) Order from disorder, corralling cholesterol with chaotic lipids. The role of polyunsaturated lipids in membrane raft formation. *Chem Phys Lipids* **132:** 79–88

Wathes DC, Abayasekara DR, Aitken RJ (2007) Polyunsaturated fatty acids in male and female reproduction. *Biol Reprod* **77:** 190–201

Williams TJ (1983) Interactions between prostaglandins, leukotrienes and other mediators of inflammation. *Br Med Bull* **39:** 239–242

Wilner GD, Nossel HL, LeRoy EC (1968) Aggregation of platelets by collagen. *J Clin Invest* **47:** 2616–2621

